



# Comparison of hot embossing micro structures with and without ultrasound

W. Zou<sup>1</sup> · J. Sackmann<sup>1</sup> · A. Striegel<sup>2</sup> · M. Worgull<sup>2</sup> · W. K. Schomburg<sup>1</sup>

Received: 18 December 2018 / Accepted: 6 May 2019 / Published online: 15 May 2019  
© Springer-Verlag GmbH Germany, part of Springer Nature 2019

## Abstract

Hot embossing with and without ultrasound are compared in this paper with respect to several properties of the fabricated samples. The same mold was employed for both processes and process parameters have been chosen adapted to each process such that to the best knowledge of the authors good moldings were achieved. Shrinkage is similar for both processes. Better mold filling is achieved without ultrasound and the polymer structures correspond better to the mold after demolding. Undesired sample curvature is also much less. With ultrasound required investment costs and energy consumption are significantly less, and the cycle time is reduced to seconds.

## 1 Introduction

Thermoplastic molding of micro structures usually is done by injection molding, hot embossing, nanoimprint or thermoforming (Giboz et al. 2007; Hecke and Schomburg 2004; Peng et al. 2014). In recent years, ultrasonic hot embossing has been developed as an alternative replication process with cycle times of a few seconds and comparatively low investment costs on the order of some 10,000 € (Altmann et al. 2012; Lee and Park 2016; Lin and Chen 2006; Liu and Dung 2005; Luo et al. 2013; Sackmann et al. 2015; Šakalys et al. 2016; Tian et al. 2014; Tseng and Lin 2012; Yu et al. 2009). The specific advantages are short cycle times and a high grade of technical flexibility, especially for prototyping. Because of the short process

times, especially heating and cooling, it was shown that the molecular structure of semi-crystalline polymers becomes amorphous by ultra-sonic hot embossing and amorphous parts are softer than semi-crystalline ones Kosloh et al. (2017).

To evaluate the performance of a replication process a comparison with a well-known process may be suitable. However, the diversity of process specific parameters makes a comparison between different replication processes challenging, because the parameters have to be set individually for each process. A comparison between injection molding and micro injection molding regarding the feature size was done by Giboz et al. (2009) analyzing the morphology of replicated structures.

In this paper, the performance of hot embossing with ultrasound was compared with the standard hot embossing process (without ultrasound). Both processes are based on an embossing cycle, but with different parameters and technologies. The comparison was reduced to measurable properties of the molded parts such as shrinkage, mold filling, sample curvature and technology features such as investment costs, required energy, and cycle time.

To perform a comparison a specific molding tool was designed used for ultrasonic hot embossing and as a mold insert for hot embossing. With this design we can compare the filling behavior, the shrinkage in lateral dimensions and quality of the shape of the replicated geometry. The replication was performed in amorphous and semi-crystalline materials, using the same polymers as semi-finished products.

✉ W. Zou  
zou@kemikro.rwth-aachen.de

J. Sackmann  
johannes.sackmann@ita.rwth-aachen.de

A. Striegel  
adrian.striegel@bmw.de

M. Worgull  
matthias.worgull@kit.edu

W. K. Schomburg  
schomburg@kemikro.rwth-aachen.de

<sup>1</sup> RWTH Aachen University, KEmikro, Campus-Boulevard 30, 52074 Aachen, Germany

<sup>2</sup> Karlsruhe Institute of Technology, Hermann-von Helmholtz-Platz 1, 76021 Karlsruhe, Germany

To achieve an irrevocable comparison, it would be necessary performing a comprehensive study of the optimum parameters of both processes and comparing the results at these parameters. However, such a work would exceed the costs affordable for the institutions of the authors and the expected outcome is not justifying this. Therefore, two research groups with experiences in these processes for many years have been working together. The process parameters of each process were set to reasonable values based on the individual technology of the replication machines. The focus is set to the replication results at reasonable conditions.

## 2 Hot embossing

Hot embossing or thermal nanoimprint is besides injection molding a well-known polymer structuring process. Because of the squeeze process hot embossing is well suited to structure surfaces down to the nanoscale even on thin thermoplastic polymer films. Typically all kinds of thermoplastic materials can be processed, starting with standard plastics like PE or PP up to high performance plastics such as, PSU, LCP, or PEEK (Worgull et al. 2011). Technical advantages of hot embossing are a comparatively short set up time and a flexible set up of the molding tool (Worgull 2009). For replication so-called mold inserts are embedded in the tool. These mold inserts can be structured by lithography processes followed by electroplating, etching processes of silicon, or mechanical machining, e.g., milling or laser ablation (Worgull 2009).

With this technical background the embossing process is a versatile process adaptable to the requirements of a number of applications, e.g., micro- and nano channels for fluidic applications, phase gratings, photonic structures (Chen 2015). Because of the short set up time the focus is set to small series or prototyping. Structures beyond typical extruded structures can also be replicated if soft mold inserts are used (Schift 2015). This kind of soft embossing or the combination of embossing with thermoforming (Schneider et al. 2014) increases the diversity of applications, e.g., surfaces with biomimetic structures characterized by hierarchical designs (Park et al. 2011; Röhrig et al.

2013). Finally the flexibility of the process in combination with the material and mold insert diversity is the strength of the embossing process.

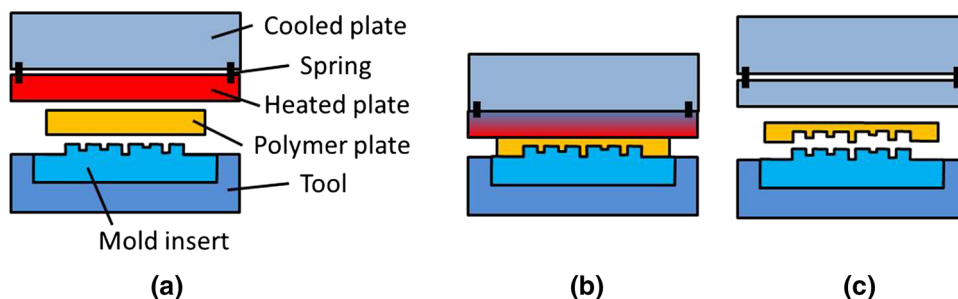
In hot embossing (without ultrasound), the tool with the micro structures on top is a so-called mold insert (Fig. 1a). This mold insert is fixed into one side of the two sided tool. The opposite part of the tool consists of a so-called substrate plate, a sand-blasted steel plate. Both, the mold insert and the substrate plate are heated and cooled by oil or water. To optimize the heating and cooling times the heating plate is separated by springs from the cooling plate. By this, an air gap of around 5 mm is achieved during heating, thermally insulating the plates from each other. The polymer is placed between mold insert and substrate plate as a foil or thin plate, typically in a range between 100 and 1500  $\mu\text{m}$  depending on the depth of the cavities. Instead of a plate, several polymer foils with the same volume can be employed yielding the same result.

The embossing cycle starts with the closing of the tool, touching the stack of mold insert, polymer foil and substrate plate. The polymer is heated up by conduction over the softening temperature into the state of a polymer melt. If the selected molding temperature is achieved a two-step embossing process is applied. Starting with a constant velocity in a range around 1 mm/min up to a selected force followed by a constant force over a certain holding time. During the application of force (velocity controlled and force controlled) the gap between heating and cooling plate is closed (Fig. 1b). By this, cooling starts immediately and reduces cycle times. Because of moderate heat conduction the polymer remains in the melt state during embossing.

After the two mold halves of the tool and within the polymer have been cooled down under the glass transition temperature, the tool is opening and the polymer is demolded from the micro structures by adhesion of the so-called residual layer on the rough substrate plate (Fig. 1c).

During hot embossing, the entire polymer is thermally cycled up to its melting state and down to demolding temperature. As a consequence, stress is generated and will be frozen after cooling resulting in shrinkage of the parts at an elevated temperature. Cooling lasts several minutes because besides the polymer also the mass of the tool needs to be cooled down. This means that a semicrystalline

**Fig. 1** Schematic drawing of hot embossing without ultrasound



polymer will recrystallize again after it had got amorphous at a temperature above its crystalline melting temperature.

If the entire polymer is heated up and molten, no difference is expected whether the polymer is placed into the machine as a single plate or a stack of foils. Inner stress in the polymer layers is released during melting and the inner stress after the process is generated by the shrinkage generated during cooling down while the polymer is enclosed in the tool at a certain pressure. For experiments, it is an advantage to place a stack of foils into the tool because, this way, it is easier to adjust the desired polymer volume by the number of foils.

In Fig. 2, there are shown three different kinds of embossing machines with different types of drive units. For high embossing forces typically a hydraulic drive system is applied, for precise controlled velocities and forces a spindle drive is recommended. Between this also an air pressure system with moderate but precise forces can be realized. Independent of the kind of construction typical costs of commercially available machines are in a range of

more than 200,000 €. Beside the few commercial available machines a number of custom made machines exist especially in labs or further adapted for serial fabrication in industry.

### 3 Ultrasonic hot embossing

For ultrasonic hot embossing, the tool is fixed on an anvil and a polymer foil and a polymer plate are placed above it (cf. Fig. 3a). Then the sonotrode of an ultrasonic welding machine is lowered onto the polymer and pressing it onto the tool. After a trigger force has been overcome, ultrasonic vibrations are induced into the sample via the sonotrode. As a consequence of the vibrations, friction heat is generated at the interface of polymer and protruding micro structures on the tool and between polymer layers. The heat is softening or even melting the polymer which is adapted to the microstructures on the tool (Fig. 3b). After approximately 1 s the ultrasound is stopped but the pressure is

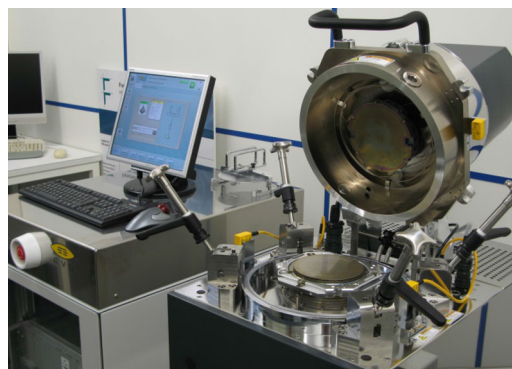
**Fig. 2** Different types of hot embossing machines optimized for different tasks. **a** Wickert WMP 1000 with a maximum embossing force of 1000 kN for large area molding. **b** Jenoptik HEX03, a multi task embossing machine with an alignment system for double sided molding. **c** EVG 510 HE, a precise pneumatic hot embossing system optimized for wafer substrates



**(a)** Wickert WMP 1000

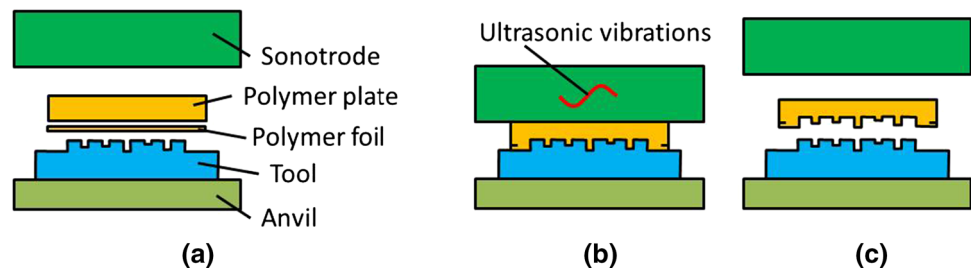


**(b)** Jenoptik HEX03



**(c)** EVG510 HE

**Fig. 3** Schematic drawing of ultrasonic hot embossing



held constant until the sample is cooled down enough for demolding (Fig. 3c). After the process, the polymer layers are joined to a single piece everywhere where they have been molten.

Since the heat is generated by ultrasonic vibrations, only the polymer and the part of the tool adjacent to it are heated up. Therefore, less energy is required for the process and cooling is achieved simply by dissipation into sonotrode and tool. As a consequence, the entire process is finished within a few seconds. Cooling down is so fast that semi-crystalline polymers become amorphous where they have been heated up during the process Kosloh et al. (2017).

Heat generation is influenced very much by the number of polymer layers, their thickness and roughness Kosloh et al. (2017). This is the reason why in general more than a single piece of polymer is placed between tool and sonotrode although that would also be possible. Employing several polymer layers results in heat generation also inside of the polymer stack and not only at the surface orientated to the tool. The surface of the sonotrode and the polymer surface facing the sonotrode are very smooth avoiding undesired heat generation. The roughness of the sonotrode is typically on the order of 1  $\mu\text{m}$ . Besides heat control, the use of several layers also facilitates molten polymer flowing sideward.

In ultrasonic hot embossing, not the entire sample is heated up resulting in anisotropic shrinkage. If a plate, 1 mm or more in thickness, is used together with a foil, some 100  $\mu\text{m}$  in thickness, only the part of the sample in the near of the tool will become heated up and is hardening again at an elevated temperature. When cooling down to room temperature, the micro patterned surface will shrink and develop tensile stress resulting in a curvature of the entire sample. If several polymer foils are employed, the sample tends to develop undulations at its rim because polymer foils are usually fabricated by extrusion and have inner stress. The inner stress is reducing locally where the foils are heated up by ultrasonic vibrations and this inhomogeneity in stress generates the undulations.

In Fig. 4, ultrasonic welding machines are shown. There are several ultrasonic welding machines on the market which can be purchased for some 10,000 €. The maximum overall size of the samples which can be machined is

limited by the available ultrasonic energy and, as a consequence, of the size of the sonotrode. The ultrasonic vibrations are generated by a stack of piezos at their resonance frequency. The resonance frequency is decreasing with increasing size of the piezos and larger piezos generate more ultrasonic power. Therefore, ultrasonic welding machines working at lower frequencies can generate more power and larger vibration amplitudes. Usually, the frequencies of ultrasonic welding machines are at 20 or 35 kHz, but other frequencies are also possible. The largest sonotrode available for the investigations described in this paper has a working area of  $80 \times 120 \text{ mm}^2$ .

## 4 Mold design

To limit the number of required experiments and molds, micro structures with several designs were placed on a single mold rather than employing several molds each with another kind of micro structures.

The mold was milled and drilled from an aluminum plate, 3, 50 and 70 mm in thickness, width and length, respectively. The mold was employed as the tool and as the mold insert for hot embossing with and without ultrasound, respectively. As shown in Fig. 5, different protruding and recessing micro structures have been milled and drilled into the surface of an aluminum plate, such as squares, cross bars, channels and cylinders. The protruding squares, 1 mm in width and length and 500  $\mu\text{m}$  in height, arranged across the mold were designed to measure the shrinkage of the molded samples parallel to both their length and width.

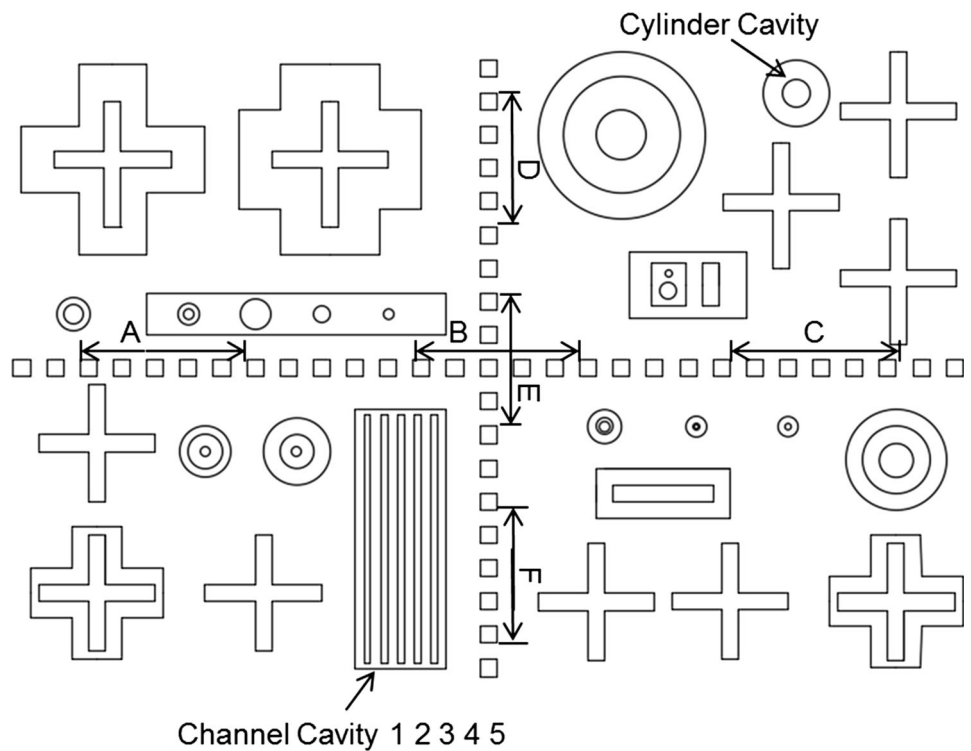
The rectangular channels and cylinder cavities were used to measure the mold filling of both processes. The cylinder hole is 1.25 mm and 1.5 mm in diameter and depth, respectively, and was drilled into the center of a protruding cylindrical plateau, 4.6 mm and 0.5 mm in diameter and height, respectively. The protruding ring, generated this way, helps filling the cylinder hole next to it by ultrasonic hot embossing because for this process the molten polymer filling a cavity in the mold needs to be generated in its nearby protruding structures displacing polymer.

The rectangular channels have been milled into a plateau elevated 500  $\mu\text{m}$  over the surrounding surface of the



Fig. 4 Ultrasonic welding machines from Herrmann Ultrasonic, Branson Ultrasonic, and Rinco Ultrasonics

Fig. 5 Technical drawing of the tool employed for hot embossing as well as ultrasonic hot embossing. The dimensions of the molded structures measured are marked in this drawing



mold providing molten polymer for filling the channels by ultrasonic hot embossing. The length and width of all channels are 13.5 mm and 250  $\mu\text{m}$ , respectively, and their depths are between 100 and 500  $\mu\text{m}$ .

The molded samples compared in this paper are marked in Fig. 5.

### 5 Experiments

Hot embossing experiments were performed with the thermoplastic polymers polycarbonate (PC), polypropylene (PP), and polyvinylidene fluoride (PVDF). The process parameters were chosen such that according to the experience of the investigators promising molding results had



**Table 1** Fabrication parameters of hot embossing experiments

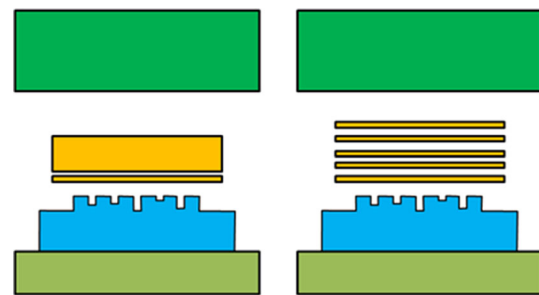
No.	Material	Cycle time (s)	Embossing force (kN)	Temperature of substrate (°C)	Temperature of mold insert (°C)	Heating energy (kJ)
1	PC	492	135	219	230	671
2	PC	488	135	218	231	683
3	PC	492	135	218	231	706
4	PP	476	100	154	154	640
5	PP	474	100	154	154	640
6	PP	498	150	153.8	154	641
7	PVDF	462	60	158.8	159	1077
8	PVDF	493	100	160.7	160	1076
9	PVDF	377	150	164.5	164	1076

been expected. The process parameters are shown in Table 1.

The theoretical minimum energy required for heating up the polymer has been calculated from the difference between room temperature (20 °C) and the temperature measured during the process and shown in Table 1, the geometrical dimensions, density and specific heat capacity are shown in Table 2. To roughly estimate the minimum energy required to heat up the tool, its diameter (232 mm) and thickness (30 mm) have been used together with density and heat capacity of aluminum 2.7 g/cm<sup>3</sup> and 0.9 J/(g K), respectively (Erbrecht et al. 2007).

Ultrasonic hot embossing experiments were performed with the thermoplastics PC, PP, and PVDF.

To investigate the influence of friction heating between several polymer layers, two different arrangements of polymer layers were employed (Fig. 6). For one of the arrangements (Fig. 6, left), a polymer foil, 500 µm in thickness, was placed on the tool. On top of that foil, there was laid a polymer plate, 4 mm in thickness. For the other arrangement (Fig. 6, right), five polymer foils, each 500 µm in thickness, were placed on the tool. The process parameters were chosen such that according to the experience of the investigators promising molding results had been expected. The required energy for heating up the polymer was directly read from the ultrasonic welding machine HiQ Dialog-Herrmann. The average process

**Fig. 6** Ultrasonic hot embossing with substrate and foil (left), and with foils

parameters of three samples with polymer foils and five samples with substrate and foil are shown in Table 3.

Figure 7 shows some microstructures fabricated by hot embossing with and without ultrasound.

## 6 Structure height ratio

In the molding thermoplastic polymers, cavities in the mold are filled by softened polymer and are demolded from them after cooling down and hardening again. The shape and height of the demolded polymer structures are influenced by all the more or less filling of the cavities, a possible deformation of a only partly hardened polymer structure during demolding, and polymer shrinkage or

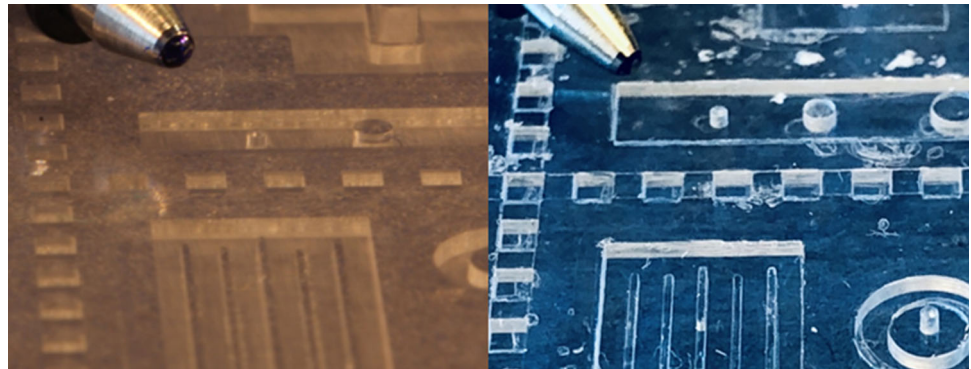
**Table 2** Geometrical and material properties of the polymers employed

Polymer	Width (mm)	Length (mm)	Height (mm)	Density (g/cm <sup>3</sup> )	Specific heat capacity [J/(g K)]
PC (Kern GmbH 2017a)	50	70	1.5	1.2	1.17
PP (polymehr GmbH 2017)	50	70	1.4	0.91	1.7
PVDF (Kern GmbH 2017b)	50	70	1.4	1.78	1.2

**Table 3** Fabrication parameters of ultrasonic hot embossing experiments

No.	Arrangement	Material	Embossing force (kN)	Amplitude (μm)	Cycle time (s)	Heating energy (kJ)
10	Five foils	PP	1.2	30.6	1.3	3.31
11	Five foils	PVDF	1.2	26.9	0.8	1.47
12	Five foils	PC	1.2	30	0.7	1.29
13	One substrate + one foil	PC	1.8	30.6	3.3	6.58

**Fig. 7** Microstructures fabricated by hot embossing with (right) and without (left) ultrasound



deformation after demolding due to cooling down and release of inner stress. Therefore, a polymer structure in general will be smaller or even may be larger than the size of the cavity in the mold.

As a consequence, it is possible that the height of a demolded polymer structure is the same as the depth of the cavity although the cavity had not been filled completely. A suitable way to prove complete mold filling is to observe whether shallow structures on the bottom of the cavity are also found on top of the demolded polymer structure (see below).

The structure height ratio SHR was defined as:

$$SHR = \frac{\text{Structure height on sample}}{\text{Structure depth on tool}} \times 100\%.$$

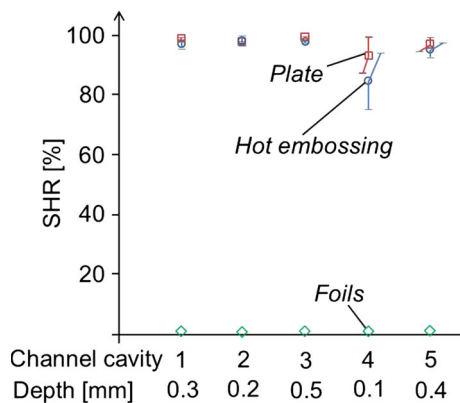


**Fig. 8** SHR of the embossings of the five channels at positions 1 through 5 (c.f. Fig. 5)

The SHR of the five channels from PC are shown in the Fig. 8. The channels in position 1–5 (Fig. 5) are 250 μm in width, 13.5 mm in length, and 0.3, 0.2, 0.5, 0.1, and 0.4 mm in depth, respectively. The channels have a distance of 1 mm to each other. Five samples were measured in each case by the microscope Eclipse LV100 from Nikon, at the center of the protruding bars on the polymer and mean value and standard deviation are shown in Fig. 8.

The average SHR of the five channels from hot embossing and ultrasonic hot embossing with substrates are 95% and 97%, respectively. The structures of the samples fabricated by ultrasonic hot embossing with substrates showed in the center of the structures a similar good mold filling as those fabricated by hot embossing.

For hot embossing it had been investigated that the air is compressed to a fraction of its volume during hot embossing and that the trapped air is not observed in the final embossed structures (Shift et al. 2001). As shown in Fig. 9a, milling marks had been generated by the milling tool at the bottom of the channels on the aluminum tool. These score marks are present on the corresponding bars fabricated by hot embossing (Fig. 9b); however, they are present only partly on the bars fabricated by ultrasonic hot embossing. It was also observed that the ends of the bars fabricated by ultrasonic hot embossing were not as high as their center parts.

That means, the channels on the tool were completely filled with molten polymer by hot embossing, but not by ultra-sonic hot embossing. The score marks on the bars

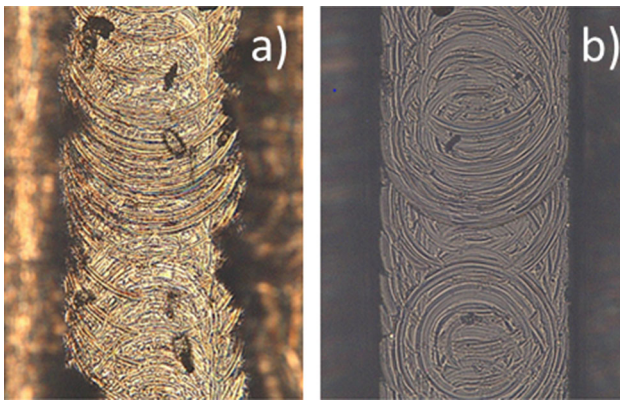


**Fig. 9** Microscopic photograph of milling marks on the bottom of the 0.1 mm wide channel on the tool (a) and on the top of a bar molded from this channel by hot embossing (b)

fabricated by hot embossing show that their height was reduced by approximately 5% because of shrinkage and not by incomplete mold filling.

No score marks were found on the bars fabricated by ultrasonic hot embossing. The incomplete filling of the samples by ultrasonic hot embossing probably is due to the cold walls of the tool resulting in polymer hardening when it enters into the narrow grooves on the tool at room temperature. It has been observed in another investigation that mold filling is improved if the tool is heated up to a temperature a bit below the softening temperature of the polymer (Sackmann et al. 2015). Heating the tool in addition to ultrasonic hot embossing was avoided in this study to make a clear distinction between hot embossing with and without ultrasound.

After ultrasonic hot embossing with foils, no clear structure could be found on the samples. Possibly the polymer was molten more by the friction heat generated between the five foils and it was squeezed out towards the sides instead of being forced into the grooves on the tool, but this cannot be proven by the experiments described here.

The SHR of the 1.5 mm deep cylinder cavity (Fig. 5) is shown in Fig. 10. The SHR of samples generated by hot

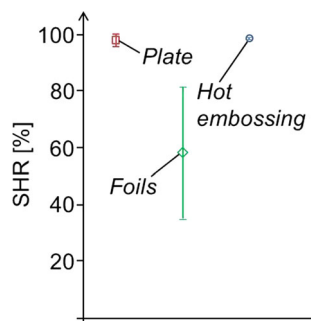


**Fig. 10** SHR of the embossings of the cylinder cavity

embossing and ultrasonic hot embossing with one foil and a plate are  $98 \pm 0.2\%$  and  $97 \pm 2.2\%$ , respectively. Similar as in the case of the molding of the five channels, score marks were completely molded on the top of the cylinders from hot embossing and not on those fabricated by ultrasonic hot embossing.

The average SHR of the samples from ultrasonic hot embossing with foils is  $58 \pm 23\%$ , which is significantly less than the result obtained with a plate and a foil.

It is concluded from these measurements that the mold filling of hot embossing was the best and nearly similar results have been obtained by ultrasonic hot embossing with a foil and a plate. However, the structures could not be well molded by ultrasonic hot embossing only with foils; especially the narrow structures were nearly not molded.

## 7 Lateral shrinkage

The shrinkage was defined as:

$$\text{Shrinkage} = \frac{\text{Tool size} - \text{Sample size}}{\text{Tool size}} \times 100\%$$

Squares indented into the samples across the tool parallel to their length and width were used to measure the lateral shrinkages of the samples. The distance over 5 and 4 squares were measured reducing measurement errors (cf. Fig. 5). Besides other structures, some of the square indentations are shown in Fig. 7. Three samples were measured in each case by the digital microscope VHX-500F from Keyence. Shrinkage and standard deviation measured of three samples in both directions are shown in Fig. 11.

The shrinkage in length direction of samples generated by hot embossing and ultrasonic hot embossing with one foil and a plate are  $0.66 \pm 0.11\%$  and  $0.79 \pm 0.17\%$ , respectively. The shrinkages in width direction are  $0.89 \pm 0.2\%$  and  $0.76 \pm 0.29\%$ , respectively. The samples fabricated by ultrasonic hot embossing with a plate showed in both directions a similar small shrinkage as those fabricated by hot embossing. The shrinkage of the five foils in general is larger.

## 8 Sample curvature

As shown in Fig. 12a, the samples fabricated by hot embossing without ultrasound are almost not curved after the process because the entire polymer has been heated up and cooled down again. Ultrasonic hot embossing with five foils resulted in undulations of the foils where they had not been exposed to the ultrasound, because they were shrinking in the center and no shrinkage occurred where



**Fig. 11** Shrinkage of the samples from PC measured parallel to their length and width fabricated by hot embossing and ultrasonic hot embossing with a plate and a foil (plate) and with five foils (foils)

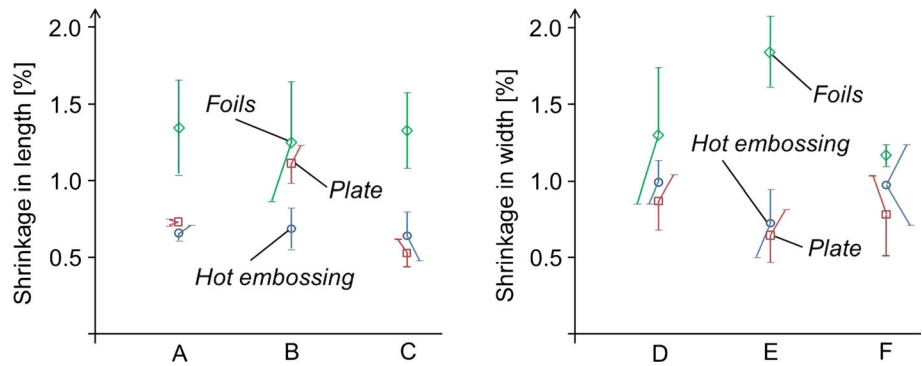
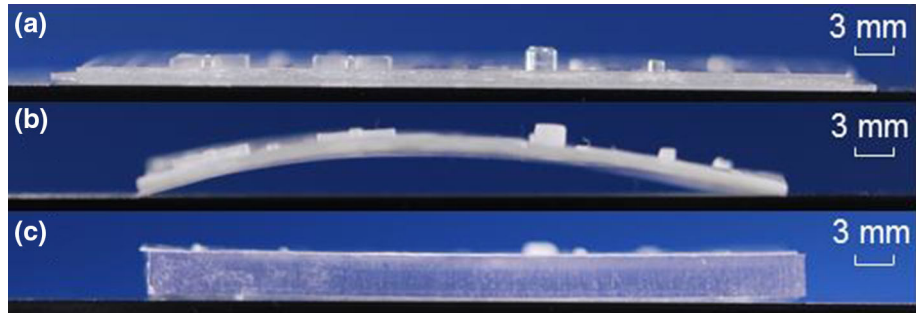


**Fig. 12** Side views of samples fabricated by hot embossing without ultrasound (a), ultrasonic hot embossing with five foils (b) and with one plate and one foil (c)



they had not been welded together at their rim. This does not need to be a problem because the rim of the samples can be cut off after ultrasonic hot embossing. However, a significant curvature is observed even after cutting away the non-welded parts (Fig. 12b).

The shrinkage of the foils when they are heated up is generated by inner stress frozen in the polymer during its fabrication. Polymer foils are fabricated by extrusion of molten polymer through a narrow slit. This way, tensile stress is generated especially in the direction of extrusion.

The inner stress in the foils in principle can be released by placing them in an oven slightly compressed between two even plates, e.g., from glass, and heating them up near to their softening temperature for approximately half an hour. It is expected that a significant reduction of the undulations after ultrasonic hot embossing can be achieved this way, but due to time constraints of the project it was not possible investigating this further.

Since only one side of a plate patterned by ultra-sonic hot embossing with a single foil is heated up, the samples fabricated this way are curved a bit (Fig. 12c). After embossing, the surface facing the tool is hotter than the rest of the polymer, and therefore, after demolding this surface is shrinking relatively to the part of the polymer which was not heated during the process. This cannot be avoided completely but reduced by preheating the plate before the process starts or by a thicker plate withstanding the stress generated on the polymer surface heated by friction in the near of the tool. The influence of preheating the plate on its

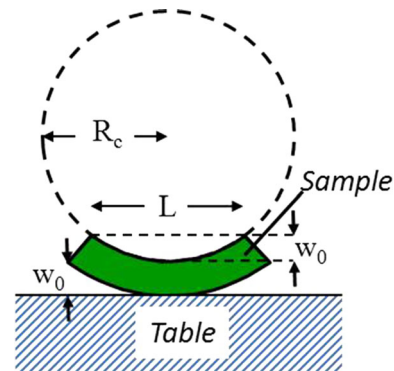


**Fig. 13** Calculation of the radius of curvature

curvature after the process has not yet been measured but is obvious.

The flexural rigidity of the plate is reducing curvature significantly. The radius of curvature  $R_c$  was calculated from a measurement of the distance  $w_0$  of the rim to an even table surface and the length  $L$  of the sample (cf. Fig. 13). The curvature of the sample is approximated by a circle. If the length of a chord of the circle is  $L$  and its maximum distance to the circle is  $w_0$ , the radius can be calculated or approximated, respectively, with the following equation (Bronstein-Semendjajew et al. 1960):

$$R_c = \frac{w_0}{2} + \frac{L^2}{8 w_0} \approx \frac{L^2}{8 w_0}. \tag{1}$$

The distance to the table was measured of three samples fabricated by ultrasonic hot embossing of a PC plate and a

PC foil according to process 13 in Table 3. Mean values and standard deviations of  $w_0$  and  $R_c$  are  $502 \pm 28 \mu\text{m}$  and  $897 \pm 51 \text{ mm}$ , respectively.

The residual stress  $\sigma_f$  of a thin film with thickness  $d_f$  on a substrate with Young's modulus  $E_s$ , thickness  $d_s$  and Poisson's ratio  $\nu_s$  is calculated from its radius of curvature by the Stoney equation (Janssen et al. 2009; Stoney 1909):

$$\sigma_f = \frac{E_s d_s^2}{6 (1 - \nu_s) R_c d_f}. \quad (2)$$

The residual stress calculated by (2) assuming  $E_s = 2.3 \text{ GPa}$ ,  $d_s = 4 \text{ mm}$ ,  $d_f = 0.5 \text{ mm}$  and  $\nu_s = 0.4$  yields a residual stress of  $22.9 \pm 1.3 \text{ MPa}$ .

If the foil had been welded at its softening temperature ( $153 \text{ }^\circ\text{C}$ ) onto the plate at room temperature, the residual stress after cooling down to room temperature ( $20 \text{ }^\circ\text{C}$ ) could be calculated as:

$$\sigma_f = E_f \alpha_{th} \Delta T = 19.3 \text{ MPa}, \quad (3)$$

where  $E_f = 2.5 \text{ GPa}$  and  $\alpha_{th} = 5.8 \cdot 10^{-5} / ^\circ\text{C}$  are Young's modulus and coefficient of thermal expansion of the foil. Besides the thermal expansion, the shrinkage of the foil due to release of inner stress is expected to generate curvature of the plate as well. The foil was fabricated by extrusion, and therefore, inner stress had been generated by its fabrication. When the foil is heated up again by ultrasonic hot embossing, this stress is released and contracting the surface of the plate. Probably, the stress causing the curvature of the samples is not only due to thermal expansion and it is expected that the curvature can be influenced by employing stress reduced foils.

## 9 Cycle time and energy consumption

As shown in Table 3, the cycle times are less than 1 s if five foils had been employed for ultrasonic hot embossing and 3.3 s if a plate was embossed together with a foil. This probably is due to the larger friction heat generated by the four interfaces between the foils compared to only one contact area between the plate and the only foil. In both cases friction heat is also expected to be generated between the protruding micro structures on the tool and the foil.

The same interpretation explains the difference in energy consumption: Ultrasonic energy is absorbed more between the five foils plus the interface between tool and the foil next to it than between the only foil and tool and plate.

For hot embossing without ultrasound, the entire polymer plus the tool are heated up and cooled down again. Therefore, the comparison of Tables 1 and 3 shows that the energy consumption is at least 100 times larger than for ultrasonic hot embossing. Compared to other fabrication

processes energy consumption is anyway small because only microscopic samples are fabricated, but the energy absorbed by polymer and tool needs to be cooled down again while the polymer is hardening inside of the tool. As a consequence, the cycle time of hot embossing without ultra-sound is at least 150 times longer.

## 10 Conclusion and discussion

Hot embossing with and without ultrasound are processes generating micro structures from thermoplastic polymers. Both processes are suitable for large-scale production (Sackmann et al. 2015; Worgull et al. 2011). The authors of this paper are aware of the fact that employing a different thermoplastic polymer or choosing improved process parameters may allow for some adjustments, but some general conclusions can be drawn:

With respect to mold filling, accuracy of the micro structures and a small substrate curvature hot embossing without ultrasound is preferable. Besides this, also there is more freedom in designing, because for ultrasonic hot embossing protruding structures in the near of a cavity need to generate the molten polymer which shall flow into it.

Mold filling by ultrasonic hot embossing is limited because the molten polymer gets into contact to a cold wall when it is entering into a cavity in the tool. Therefore, it tends to harden quickly and cannot fill cavities with a high aspect ratio. Sackmann et al. have shown that mold filling can be improved when the tool is heated up near to its softening temperature for ultrasonic hot embossing (Sackmann et al. 2015). Since this is similar to a combination of hot embossing with and without ultrasound, tool heating was not used in the study described here.

With respect to shrinkage, no significant differences were found between the three processes investigated. Shrinkage is also a function of the design of substrate and micro structures and some designs may work better with one of the processes while others may show a smaller shrinkage with a different process.

With respect to investment and fabrication costs, ultrasonic hot embossing has large advantages because the required machines require approximately five times less investment costs and the cycle times are approximately 100 times shorter. Besides this, the ultrasonic machines can also be employed for ultrasonic welding building up more complicated devices from the embossed structures (Sackmann et al. 2015).

Therefore, as a function of the application, hot embossing with or without ultrasound will be the better option.

## References

- Altmann B, Ahrens R, Welle A, Dinglreiter H, Schneider M, Schober A (2012) Microstructuring of multiwell plates for three-dimensional cell culture applications by ultrasonic embossing. *Biomed Microdevice* 14:291–301. <https://doi.org/10.1007/s1054401196058Y>
- Bronstein-Semendjajew (1960) Taschenbuch der Mathematik. Verlag Harri Deutsch, Leipzig. ISBN 3-87144-016-7
- Chen Y (2015) Applications of nanoimprint lithography/hot embossing: a review. *Appl Phys A* 121:451–465. <https://doi.org/10.1007/s00339-015-9071-x>
- Erbrecht R, Felsch M, König H et al (2007) Das große Tafelwerk: interaktiv. Cornelsen Verlag, Berlin (1.Auflage 10.Druck). ISBN 978-3-464-57144-6
- Giboz J, Copponnex T, Mélé P (2007) Microinjection molding of thermoplastic polymers: a review. *J Micromech Microeng* 17:R96–R109. <https://doi.org/10.1088/0960-1317/17/6/R02>
- Giboz J, Copponnex T, Mélé P (2009) Microinjection molding of thermoplastic polymers: morphological comparison with conventional injection molding. *J Micromech Microeng* 19:025023. <https://doi.org/10.1088/0960-1317/19/2/025023>
- Heckele M, Schomburg WK (2004) Review on micro molding of thermoplastic polymers. *J Micromech Microeng* 14:R1–R14. <https://doi.org/10.1088/0960-1317/14/3/R01>
- Janssen GCAM, Abdalla MM, van Keulen F, Pujada BR, van Venrooy B (2009) Celebrating the 100th anniversary of the Stoney equation for film stress: developments from polycrystalline steel stripes to single crystal silicon wafers. *Thin Solid Films* 517:1858–1867. <https://doi.org/10.1016/j.tsf.2008.07.014>
- Kern GmbH (2017a) Technisches Datenblatt: Polycarbonat. [https://www.kern.de/de/technisches-datenblatt/polycarbonat-pc?n=2301\\_1](https://www.kern.de/de/technisches-datenblatt/polycarbonat-pc?n=2301_1). Accessed 17 July 2017
- Kern GmbH (2017b) Technisches Datenblatt: Polyvinylidenfluorid. [https://www.kern.de/de/technisches-datenblatt/polyvinylidenfluorid-pvdf?n=1651\\_1](https://www.kern.de/de/technisches-datenblatt/polyvinylidenfluorid-pvdf?n=1651_1). Accessed 17 July 2017
- Kosloh J, Sackmann J, Schomburg WK (2017a) Ultrasonic fabrication of micro fluidic channels from polyether ether ketone (PEEK). *Microsyst Technol* 23:5505–5513. <https://doi.org/10.1007/s00542-017-3284-1>
- Kosloh J, Sackmann J, Šakalys R, Liao S, Gerhardy C, Schomburg WK (2017b) Heat generation and distribution in the ultrasonic hot embossing process. *Microsyst Technol* 23:1411–1451. <https://doi.org/10.1007/s00542-016-2836-0>
- Lee H-J, Park K (2016) Variable wettability control of a polymer surface by selective ultrasonic imprinting and hydrophobic coating. *Colloid Polym Sci* 294:1413–1423. <https://doi.org/10.1007/s00396-016-3902-y>
- Lin C, Chen R (2006) Ultrasonic nanoimprint lithography: a new approach to nanopatterning. *J Micro Nanolithography MEMS MOEMS* 5:011003. <https://doi.org/10.1117/1.2172992>
- Liu S-J, Dung Y-T (2005) Hot embossing precise structure onto plastic plates by ultrasonic vibration. *Polym Eng Sci* 45:915–925. <https://doi.org/10.1002/pen.20357>
- Luo Y, Yan X, Qi N, Wang X, Wang L (2013) Study of double-side ultrasonic embossing for fabrication of microstructures on thermoplastic polymer substrates. *PLoS One* 8(4):e61647. <https://doi.org/10.1371/journal.pone.0061647.g003>
- Park YM, Gang M, Seo YH, Kim BH (2011) Artificial petal surface based on hierarchical micro- and nanostructures. *Thin Solid Films* 520:362–367. <https://doi.org/10.1016/j.tsf.2011.07.013>
- Peng L, Deng Y, Yi P, Lai X (2014) Micro hot embossing of thermoplastic polymers: a review. *J Micromech Microeng* 24:013001. <https://doi.org/10.1088/0960-1317/24/1/013001>
- polymehr GmbH (2017) Technisches Datenblatt: Polypropylen. <https://www.polymehr.com/wp-content/uploads/technisches-datenblatt-pp.pdf>. Accessed 17 July 2017
- Röhrig M, Schneider M, Etienne G, Oulhadj F, Pfannes F, Kolew A, Worgull M, Hölscher H (2013) Hot pulling and embossing of hierarchical nano- and micro-structures. *J Micromech Microeng* 23:105014. <https://doi.org/10.1088/0960-1317/23/10/105014>
- Sackmann J, Burlage K, Gerhardy C, Memering B, Liao S, Schomburg WK (2015) Review on ultrasonic fabrication of polymer micro devices. *Ultrasonics* 56:189–200. <https://doi.org/10.1016/j.ultras.2014.08.007>
- Šakalys R, Janušas G, Palevičius A, Čekas E, Jūrėnas V, Sodah A (2016) Microstructures replication using high frequency excitation. *Microsyst Technol* 22:1831–1843. <https://doi.org/10.1007/s00542-016-2858-7>
- Schift H (2015) Nanoimprint lithography: 2D or not 2D? A review. *Appl Phys A* 121:415–435. <https://doi.org/10.1007/s00339-015-9106-3>
- Schneider N, Zeiger C, Kolew A, Schneider M, Leuthold J, Hölscher H, Worgull M (2014) Nanothermoforming of hierarchical optical components utilizing shape memory polymers as active molds. *Opt Mater Express* 4:1895–1902. <https://doi.org/10.1364/OME.4.001895>
- Shift H, Heyderman LJ, Auf der Maur M, Gobrecht J (2001) Pattern formation in hot embossing of thin polymer films. *Nanotechnology* 12:173–177. <https://doi.org/10.1088/0957-4484/12/2/321>
- Stoney GG (1909) The tension of metallic films deposited by electrolysis. *Proc R Soc Lond A* 82:172–175
- Tian W, Huang L, Wang D, Roy VAL (2014) A general, rapid and solvent-free approach to fabricating nanostructured polymer surfaces. *Sci China Technol Sci* 57:2328. <https://doi.org/10.1007/s11431-014-5647-5>
- Tseng P, Lin C (2012) Impacts of mold material and pattern size for ultrasonic nanoimprint lithography. *Microelectron Eng* 98:112. <https://doi.org/10.1016/j.mee.2012.07.083>
- Worgull M (2009) Hot embossing: theory and technology of microreplication. Elsevier, Amsterdam. ISBN 978-0-8155-1579-1
- Worgull M, Kolew A, Heilig M, Schneider M, Dinglreiter H, Rapp B (2011) Hot embossing of high performance polymers. *Microsyst Technol* 17:585–592. <https://doi.org/10.1007/s00542-010-1155-0>
- Yu HW, Lee CH, Jung PG, Shin BS, Kim J-H, Hwang K-Y, Ko JS (2009) Polymer microreplication using ultrasonic vibration energy. *J Micro Nanolithography MEMS MOEMS* 8(2):021113. <https://doi.org/10.1117/1.3129824>

**Publisher's Note** Springer Nature remains neutral with regard to jurisdictional claims in published maps and institutional affiliations.